Available online at www.sciencedirect.com
SCIENCE DIRECT®
Journal of Organometallic Chemistry 676 (2003) 62–72
Journal of Organometallic Chemistry
www.elsevier.com/locate/jorganchem

Electrochemistry of ferrocenylphosphines $FcCH_2PR_2$ (Fc = (η^5-C_5H_5)Fe(η^5-C_5H_4); R = Ph, CH_2OH and CH_2CH_2CN), and some phosphine oxide, phosphine sulfide, phosphonium and metal complex derivatives

Alison J. Downard [a,*], Nicholas J. Goodwin [b], William Henderson [b]

[a] Department of Chemistry, University of Canterbury, Private Bag 4800, Christchurch, New Zealand
[b] Department of Chemistry, University of Waikato, Private Bag 3105, Hamilton, New Zealand

Received 6 March 2003; received in revised form 6 March 2003; accepted 17 April 2003

Abstract

Electrochemical studies of the free ferrocenylphosphine ligands $FcCH_2PR_2$ (Fc = (η^5-C_5H_5)Fe(η^5-C_5H_4); R = Ph, CH_2OH and CH_2CH_2CN) and some phosphine oxide, phosphine sulfide, phosphonium and metal derivatives are described. The free ligands exhibit complex voltammetric responses due to participation of the phosphorus lone pair in the redox reactions. Uncomplicated ferrocene-based redox chemistry is observed for P^V derivatives and when the ligands are coordinated in complexes *cis*-$PtCl_2[FcCH_2P(CH_2OH)_2]$, $PdCl_2[FcCH_2P(CH_2OH)_2]$, $[Au\{FcCH_2P(CH_2OH)_2\}_2]Cl$, $RuCl_2(\eta^6$-$C_{10}H_{14})[FcCH_2P(CH_2OH)_2]$ and $RuCl_2(\eta^6$-$C_{10}H_{14})(FcCH_2PPh_2)$. The reaction pathways of the free ligands after one-electron oxidation have been examined in detail using voltammetry, NMR spectroscopy and electrospray mass spectrometry. Direct evidence for formation of a P–P bonded product is presented.

Keywords: Ferrocenyl group; Phosphine; Electrochemistry; NMR spectroscopy; Ferrocenium reaction

1. Introduction

One of the best known properties of ferrocenes is their ability to undergo reversible one-electron oxidation. Adding a phosphine sustituent to the ferrocene allows incorporation of the redox-active ferrocenyl moiety into transition metal complexes, often leading to an increase in the reactivity of the complex. Coordinated ferrocenylphosphine ligands usually exhibit simple, reversible electrochemistry arising from one-electron oxidation of the ferrocene center [1]. This well-behaved redox chemistry accounts, in part, for their popularity as ligands. In contrast, free ferrocenylphosphine ligands typically display quite complex redox chemistry which is attributed to involvement of the P^{III} lone pair electrons.

1,1'-bis(Diphenylphosphino)ferrocene (dppf) is the most widely used and studied ferrocenylphosphine ligand. The electrochemistry of the free ligand [2– and of a large number of metal complexes of dppf have been reported [1], however, only Pilloni et al. [2] have examined the electrochemistry of dppf in detail. Comments have also been made concerning the electrochemistry of other ferrocenylphosphine ligands in which the phosphine moiety is directly linked to a cyclopentadienyl ring; their redox chemistry appears to be qualitatively similar to that of dppf [8– . Recently new synthetic routes to ferrocenylmethylphosphine ligands [Fe(η^5-C_5H_5){η^5-$C_5H_4CH_2PR_2$}] ($FcCH_2PR_2$) [18– and $FcCH(CH_3)PR_2$ [23] have been developed leading to the synthesis of series of compounds with a carbon spacer between the cyclopentadienyl ring and the P atom. The reactivities and complexation chemistry of

* Corresponding author. Tel.: +64-3-364-2501; fax: +64-3-364-2110.
E-mail address: a.downard@chem.canterbury.ac.nz (A.J. Downard).

0022-328X/03/$ - see front matter © 2003 Elsevier Science B.V. All rights reserved.
doi:10.1016/S0022-328X(03)00309-7

$FcCH_2PR_2$ (R = H, CH_2OH, CH_2CH_2CN and Ph) have been investigated [18,24,25] and some chemistry of $FcCH(CH_3)PR_2$ (R = CH_2OH, CH_2CH_2CN and $CH_2(NC_4H_8O)$) has been established [26,27]. However, there are few reports concerning the redox properties of these compounds. The oxidation potential of $FcCH_2P(O)(OCH_3)OH$ has been reported [28], and of $FcCH_2P(CH_2OH)_2$, $FcCH_2P(O)(CH_2OH)_2$ and $FcCH_2P(S)(CH_2OH)_2$ attached to silicon surfaces [29]. In the latter study each compound exhibited a chemically reversible oxidation process which was attributed to the ferrocenyl moiety, however, the ferrocenyl layers were not stable to repeat redox cycling. Most recently, gold and silver complexes of $FcCH_2PPh_2$ were found to exhibit reversible one-electron electrochemistry based on the ferrocenyl moiety, and the redox chemistry of the free ligand was reported to resemble that of dppf [25].

In this work, we expand the study of the electrochemistry of ferrocenylmethylphosphine ligands to include $FcCH_2P(CH_2OH)_2$, $FcCH_2P(CH_2CH_2CN)_2$ and some phosphine oxide, phosphine sulfide and phosphonium derivatives. Several palladium, platinum and ruthenium complexes of the ligands are also examined. A detailed investigation of the redox chemistry of the free ligands using bulk electrolysis, ^{31}P NMR and electrospray mass spectrometry (ESMS) reveals some similarities and some important differences to the redox chemistry of dppf.

2. Results

2.1. Cyclic voltammetry of ferrocenylphosphines $FcCH_2PPh_2$, $FcCH_2P(CH_2OH)_2$ and $FcCH_2P(CH_2CH_2CN)_2$

Fig. 1 shows cyclic voltammograms of $FcCH_2PPh_2$, $FcCH_2P(CH_2OH)_2$ and $FcCH_2P(CH_2CH_2CN)_2$ recorded at scan rate = 100 mV s^{-1}. Electrochemical data are given in Table 1; unless noted, identical electrochemical behaviour was observed using Pt and glassy carbon (GC) working electrodes. ^{31}P NMR data are also included in Table 1 for convenience.

All ferrocenylphosphines show a major oxidation process near 0 V vs FcH^+/FcH followed by a second process with lower current at ca. 200 mV higher potential. Under the experimental conditions of Fig. 1, the second process is very minor for $FcCH_2P(CH_2CH_2CN)_2$ but it is more significant at lower scan rate or higher concentration. When the potential is scanned in the negative direction after first traversing the oxidation steps, one ($FcCH_2PPh_2$ and $FcCH_2P(CH_2CH_2CN)_2$) or two ($FcCH_2P(CH_2OH)_2$) broad, irreversible reduction peaks of relatively low current are observed at potentials between −1.3 and −1.7 V. These peaks are absent in scans commencing in the negative direction. Cyclic voltammograms of the compounds recorded in dichloromethane solution show the same features except that the second oxidation peak for $FcCH_2P(CH_2OH)_2$ is small and sharp and there is an associated large and sharp cathodic peak indicative of adsorbed species. Considering the major oxidation peak, there is a linear relationship between the anodic peak current, i_{pa1}, and (scan rate)$^{1/2}$ over the range 20–500 mV s^{-1} indicating a diffusion controlled process. Comparison of the responses with that of equimolar $FcCH_2P(O)(CH_2OH)_2$ under the same conditions (see below) enables the process to be assigned to the transfer of one-electron. Based on the observed $E_{1/2}$ values and the redox chemistry of other ferrocenylphosphines, the first oxidation peak is assumed to correspond to oxidation of the ferrocenyl moiety. $E_{1/2}$ values are negative of the FcH^+/FcH couple, consistent with the electron donating effect of the methylene substituent.

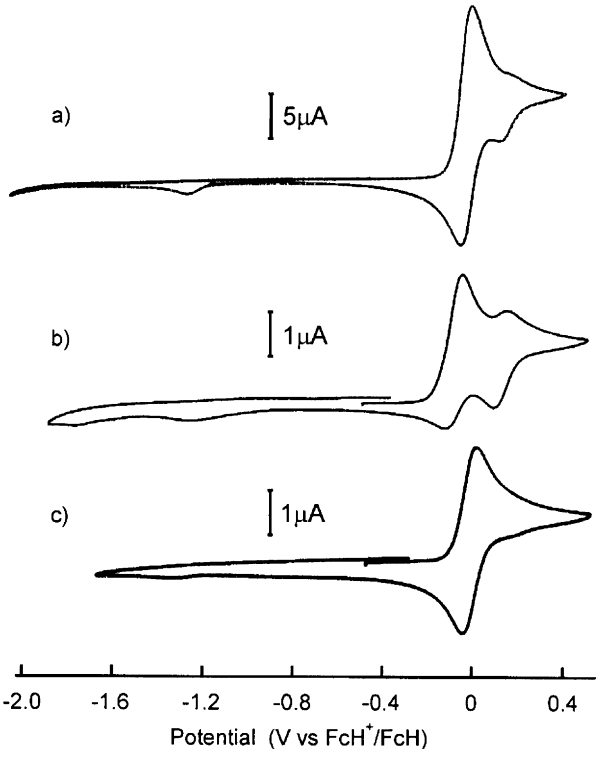

Fig. 1. Cyclic voltammograms obtained using a Pt disk electrode, scan rate = 100 mV s^{-1} of (a) 7.5 mM $FcCH_2PPh_2$, (b) 1 mM $FcCH_2P(CH_2OH)_2$ and (c) 1 mM $FcCH_2P(CH_2CH_2CN)_2$.

For all compounds the chemical reversibility of the major oxidation process depends on the concentration and potential scan rate. As shown in Fig. 2 for $FcCH_2P(CH_2OH)_2$, the cathodic to anodic peak current ratio for the first oxidation process decreases with decrease in scan rate and with increase in concentration from 0.5–5 mM. The current for the second oxidation peak relative to the first increases with decreasing scan rate and increasing concentration, reaching a maximum of 0.5 at slow scan rate and high concentration (Fig. 2d).

Table 1
Cyclic voltammetric and ^{31}P NMR data for ferrocenylphosphines, phosphine oxides, sulfides and metal complexes

Compound	E_{pa1}	E_{pc1}	$E_{1/2(1)}$	E_{pa2}	E_{pc2}	$E_{1/2(2)}$	E_{pc} [a]	Chemical shift (δ) [b]
$FcCH_2PPh_2$	0	−0.07	−0.04	0.20	0.11	0.16	−1.2 [c]	−11.8
$FcCH_2P(CH_2CH_2CN)_2$	0.03	−0.06	−0.02	0.22	0.14	0.18	−1.3 [c]	−22.1
$FcCH_2P(CH_2OH)_2$	−0.03	−0.11	−0.07	0.16	0.10	0.13	−1.4 [c], −1.7 [c]	−19.3
$FcCH_2P(O)(CH_2OH)_2$	0.04	−0.03	0					45.8
$FcCH_2P(S)(CH_2OH)_2$	0.05	−0.03	0.01					44.0
$FcCH_2P(O)Ph_2$	0.06	−0.01	0.02					29.0
$[(FcCH_2)_2P(CH_2OH)_2]Cl$	0.17	0.08	0.13				−2.7 [d], −1.5 [e]	22.30 [f]
$[FcCH_2P(Bz)(CH_2OH)_2]Br$	0.15	0.08	0.12				−2.7 [d], −1.6 [e]	26.0 [f]
$[FcCH_2P(H)Ph_2]BF_4$	0.17	0.11	0.14				−1.3 [c,d], −1.9 [d] −0.8 [e], −1.3 [c,e]	6.31
cis-$PtCl_2[FcCH_2P(CH_2OH)_2]$	0.07	−0.02	0.03					7.8 [f]
$PdCl_2[FcCH_2P(CH_2OH)_2]$	0.08	0	0.04					32.4 [f]
$[Au\{FcCH_2P(CH_2OH)_2\}_2]Cl$	0.09	0.01	0.05					36.2 [f]
$RuCl_2(\eta^6\text{-}C_{10}H_{14})[FcCH_2P(CH_2OH)_2]$	0.04	−0.03	0.01	0.76	0.66	0.71		25.9
$RuCl_2(\eta^6\text{-}C_{10}H_{14})(FcCH_2PPh_2)$	−0.09	−0.15	−0.12	0.71	0.58	0.64		28.8

CH_3CN–0.1 M $[Bu_4N]BF_4$ or $[Bu_4N]PF_6$; scan rate = 100 mV s^{-1}; potentials are in V vs FcH^+/FcH; except where noted, potentials are independent of electrode material.

[a] Broad irreversible peak.

[b] Unless noted otherwise, solvent is $CDCl_3$.

[c] Only present after scanning through oxidation processes.

[d] GC electrode.

[e] Pt electrode.

[f] d^6-DMSO.

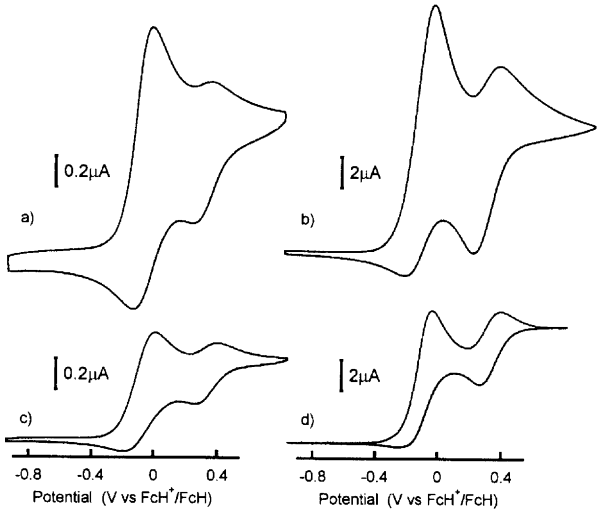

Fig. 2. Cyclic voltammograms obtained using a Pt disk electrode of (a), (c) 0.5 mM $FcCH_2P(CH_2OH)_2$ and (b), (d) 5 mM $FcCH_2P(CH_2OH)_2$. (a), (b) Scan rate = 100 mV s^{-1}; (c), (d) scan rate = 20 mV s^{-1}.

These results are consistent with a mechanism based on a bimolecular reaction involving the initially formed ferrocenium to give products which can be reversibly oxidized at a more positive potential and irreversibly reduced at quite negative potentials (an ECE mechanism). The relative reaction rates of the oxidized ferrocenylphosphines can be deduced from the currents for the second oxidation peak (at constant concentration and scan rate) and appear to increase in the order: $FcCH_2PPh_2 \approx FcCH_2P(CH_2CH_2CN)_2 < FcCH_2P(CH_2OH)_2$.

In order to gain more insight into the reaction pathway, attempts were made to simulate the cyclic voltammetry of $FcCH_2P(CH_2OH)_2$ using the DIGISIM software package (Bioanalytical Systems) [30]. A variety of mechanisms were considered and calculated voltammograms were compared with those obtained at 22 °C using 0.5–5 mM $FcCH_2P(CH_2OH)_2$ and scan rates ranging from 20–500 mV s^{-1}. Despite extensive efforts, a good match between experimental and calculated voltammograms could not be obtained, suggesting a more complex system than is apparent from casual inspection of the voltammograms.

2.2. Cyclic voltammetry of ferrocenylphosphine oxides $FcCH_2P(O)Ph_2$ and $FcCH_2P(O)(CH_2OH)_2$ and sulfide $FcCH_2P(S)(CH_2OH)_2$

The phosphine oxides and sulfide exhibit a simple, chemically reversible one-electron oxidation process with $E_{1/2}$ values slightly positive that of FcH^+/FcH (Table 1). There are no other redox processes within the solvent limit. The one-electron nature of the redox change is assigned by comparison of the current with that for oxidation of equimolar ferrocene. The cyclic voltammetric ΔE_p values are in the range 65–74 mV as found for oxidation of ferrocene under the same conditions (scan rate = 100 mV s^{-1}; concentration ~1 mM). Thus, it is assumed that the electron transfer is

reversible and that there is a contribution to ΔE_p from uncompensated solution resistance.

For each of these compounds the electron transfer step is located on the ferrocenyl moiety. The potentials of the redox processes are typical for oxidation of ferrocene derivatives [1,28] and it is well known that phosphine oxides and sulfides cannot undergo phosphine-based oxidations at low potentials [31]. As found for other ferrocenylphosphine compounds, formation of a P^V center appears to prevent follow-up chemical reactions of the ferrocenium [8,9,13,14]. The more positive $E_{1/2}$ values compared with the parent ferrocenylphosphines are attributed to the relative electron withdrawing properties of P^{III} and P^V.

2.3. Cyclic voltammetry of the ferrocenylphosphonium salts $[FcCH_2P(Bz)(CH_2OH)_2]Br$, $[FcCH_2P(H)Ph_2]BF_4$ and $[(FcCH_2)_2P(CH_2OH)_2]Cl$

Cyclic voltammograms of $[FcCH_2P(Bz)(CH_2OH)_2]Br$ and $[FcCH_2P(H)Ph_2]BF_4$ show a reversible one-electron oxidation couple. For $[(FcCH_2)_2P(CH_2OH)_2]Cl$ the peak currents are approximately doubled and there is a slight broadening of the peaks arising from two very closely-spaced couples. $E_{1/2}$ values for the phosphonium oxidations are between 0.12 and 0.14 V vs FcH^+/FcH (Table 1). For all compounds, the oxidation is assigned to the ferrocene/ferrocenium couple. As expected, there are no chemical complications due to involvement of the P^V center but the positive charge of the phosphonium shifts the $E_{1/2}$ values are significantly positive compared with those for the phosphine oxides and sulfide. Phosphoniums $[FcCH_2P(Bz)(CH_2OH)_2]Br$ and $[(FcCH_2)_2P(CH_2OH)_2]Cl$ also exhibit an irreversible reduction peak at $E_{pc} = -2.7$ V (GC electrode) and ~ -1.5 V (Pt electrode), scan rate = 100 mV s^{-1}. By comparison with the oxidation peak currents, these reductions appear to involve the transfer of one-electron although definitive assignment is not possible due to the broadness of the peaks. These processes are assigned to phosphonium reduction. As shown in Fig. 3, scanning through the reduction process gives rise to a small peak ~ 200 mV less positive than the major oxidation process. The new peak is at a similar potential to the parent ferrocenylphosphine consistent with the expected reductive cleavage of the phosphoniums to yield phosphines [32]. The reason for the strong dependence of the reduction peak potential on electrode material is not understood and was not investigated further. However, it is interesting to note that very similar behaviour was observed for the reduction of $FcCH_2NMe_2H^+$ at Au, Pt and GC electrodes [33]. The reductive electrochemical response is more complex for $[FcCH_2P(H)Ph_2]BF_4$. Broad irreversible reduction peaks are seen at $E_{pc} = -1.9$ V (GC electrode) and -0.8 V (Pt electrode), scan rate = 100 mV s^{-1}. These processes appear analogous to those described for $[FcCH_2P(Bz)(CH_2OH)_2]Br$ and $[(FcCH_2)_2P(CH_2OH)_2]Cl$. In addition, after scanning through the oxidation peak of $[FcCH_2P(H)Ph_2]BF_4$ a small irreversible reduction peak with low current appears at $E_{pc} = -1.3$ V. This most likely has the same origin as the irreversible reduction process observed for $FcCH_2PPh_2$ suggesting that oxidation of $[FcCH_2P(H)Ph_2]BF_4$ and $FcCH_2PPh_2$ leads to the same product(s).

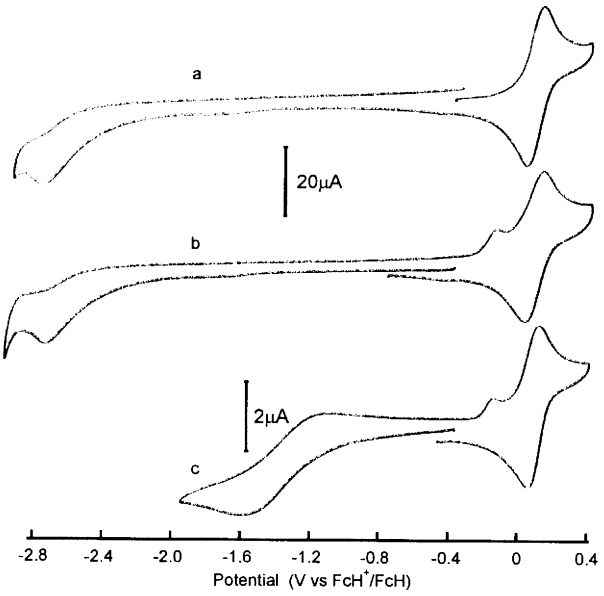

Fig. 3. Cyclic voltammograms obtained using a Pt disk electrode of 1 mM $[(FcCH_2)_2P(CH_2OH)_2]Cl$. (a), (b) GC electrode, scan rate = 200 mV s^{-1} and (c) Pt disk electrode, scan rate = 200 mV s^{-1}.

2.4. Cyclic voltammetry of ferrocenylphosphine complexes cis-$PtCl_2[FcCH_2P(CH_2OH)_2]$, $PdCl_2[FcCH_2P(CH_2OH)_2]$, $[Au\{FcCH_2P(CH_2OH)_2\}_2]Cl$, $RuCl_2(\eta^6\text{-}C_{10}H_{14})[FcCH_2P(CH_2OH)_2]$ and $RuCl_2(\eta^6\text{-}C_{10}H_{14})(FcCH_2PPh_2)$

The Pt(II), Pd(II) and Au(I) complexes of $FcCH_2P(CH_2OH)_2$ have simple, clean electrochemistry in acetonitrile solution. All complexes exhibit a single reversible oxidation process with $E_{1/2}$ slightly positive of FcH^+/FcH (Table 1). As observed for other ferrocenylphosphine metal complexes, involvement of the phosphorus lone pair in coordination to the metal shuts down the chemical complications seen for the free ligands giving ferrocenyl-based redox processes [1,10,15,25,34]. The observation of a single redox process for $[Au\{FcCH_2P(CH_2OH)_2\}_2]Cl$ which has two ferrocenylphosphine ligands indicates that interaction between the ferrocene groups is very small. The Ru(II) complexes of $FcCH_2P(CH_2OH)_2$ and $FcCH_2PPh_2$ exhibit a reversible one-electron oxidation process at low potentials followed by a second oxidation process

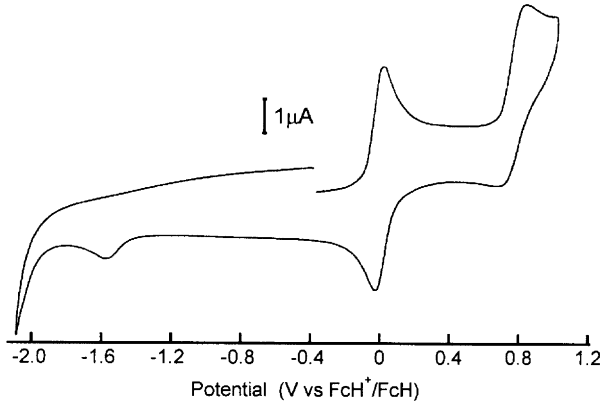

Fig. 4. Cyclic voltammogram obtained using a Pt disk electrode, scan rate = 200 mV s^{-1} of 0.9 mM $RuCl_2(\eta^6\text{-}C_{10}H_{14})(FcCH_2PPh_2)$.

at higher potentials which is not fully chemically reversible at scan rates ≤ 500 mV s^{-1} (Fig. 4). The first redox process is assumed to be ferrocene-based, and the second due to oxidation of the Ru(II) center.

2.5. Bulk electrolysis with ^{31}P NMR analysis of the redox products of $FcCH_2PPh_2$ and $FcCH_2P(CH_2OH)_2$

The cyclic voltammetry described above strongly suggests that the complexity seen in the electrochemistry of the free ferrocenylphosphines is due to the presence of the P^{III} center with its lone pair of electrons. In order to further probe the redox chemistry, detailed investigations using bulk electrolysis with voltammetric and ^{31}P NMR analysis of reaction products were undertaken. Results for these experiments are given in Table 2.

Controlled potential and controlled current bulk electrolyses of $FcCH_2PPh_2$ and $FcCH_2P(CH_2OH)_2$ were performed in acetonitrile −0.1 M $[Bu_4N]BF_4$ solutions. When investigating the first oxidation step, controlled potential electrolyses were undertaken at an applied potential between the first and second oxidation process. After passing the same amount of charge, results were identical for controlled potential and controlled current electrolyses and hence the more rapid controlled current method was usually preferred. Most studies were based on $FcCH_2PPh_2$ which showed clean formation of reaction products compared with more complex behaviour for $FcCH_2P(CH_2OH)_2$. Electrolyses were performed using 1 and 5 mM solutions of the ferrocenylphosphine; monitoring of the electrolyses by cyclic voltammetry and steady state voltammetry showed that the results did not depend on concentration and hence 5 mM ferrocenylphosphine was used to facilitate rapid ^{31}P NMR analysis of the electrolysis solutions. Rapid analysis was important because irreversible changes in solution composition were seen over the course of 1 h. For comparison, bulk electrolyses were also performed in dichloromethane and DMF yielding very similar voltammetric and ^{31}P NMR data to those obtained in acetonitrile solutions.

Controlled current oxidation of $FcCH_2PPh_2$ in acetonitrile solution by a charge corresponding to 1 F mol^{-1} results in a golden solution with a green tint. Voltammetric changes during the electrolysis are shown in Fig. 5Aa–d. There is a progressive decrease in the current due to the main oxidation peak and after oxidation by one-electron, a broad peak, (labelled (i) in Fig. 5Ad) with low current is observed at ~ 0 V. Concomitantly, there is an increase in current due to a reversible oxidation process with $E_{1/2} = 0.15$ and an irreversible reduction with $E_{pc} = -1.25$ V. These are labelled (ii) and (iii), respectively in Fig. 5Ad. Comparison of Fig. 5Ac and d shows that when the potential scan is initiated in the negative direction first and traverses peak (iii), the current at (i) is larger than when the scan is initiated in the positive potential direction. Evidently a species oxidized at (i) is generated by reduction process (iii). The potentials of the reversible couples (i) and (ii) suggest ferrocene-based electron transfers; steady-state voltammetry at a microelectrode electrode shows that in the oxidized solution, the ferrocene centers are at least 90% in the neutral (non-oxidized) form. When the oxidized bulk electrolysis solution is briefly reduced at −0.4 V (charge passed is less than 0.1 F mol^{-1}) prior to obtaining the steady

Table 2
Cyclic voltammetric and ^{31}P NMR data for products formed by oxidative bulk electrolysis of $FcCH_2PPh_2$ and $FcCH_2P(CH_2OH)_2$

Starting compound	E_{pa1}	E_{pc1}	$E_{1/2(1)}$	E_{pa2}	E_{pc2}	$E_{1/2(2)}$	E_{pc} [a]	Chemical shift (δ)
$FcCH_2PPh_2$	0.03	−0.03	0	0.18	0.11	0.15	−1.25	22.7, 23.6 ($J = 118$ Hz) 108.2, 109.1 ($J = 118$ Hz)
$FcCH_2P(CH_2OH)_2$	0.04	−0.03	0.01	0.13	0.07	0.10	−1.6 [b], −1.8 [b] −1.4 [c], −1.8 [c]	21.9, 22.7 ($J = 103$ Hz) 24.1 114.8, 115.6 ($J = 102$ Hz)

CH_3CN–0.1 M $[Bu_4N]BF_4$; voltammetry: scan rate = 100 mV s^{-1}; potentials are in V vs FcH^+/FcH; except where noted, potentials are independent of electrode material.

[a] Irreversible peak.

[b] GC electrode.

[c] Pt electrode.

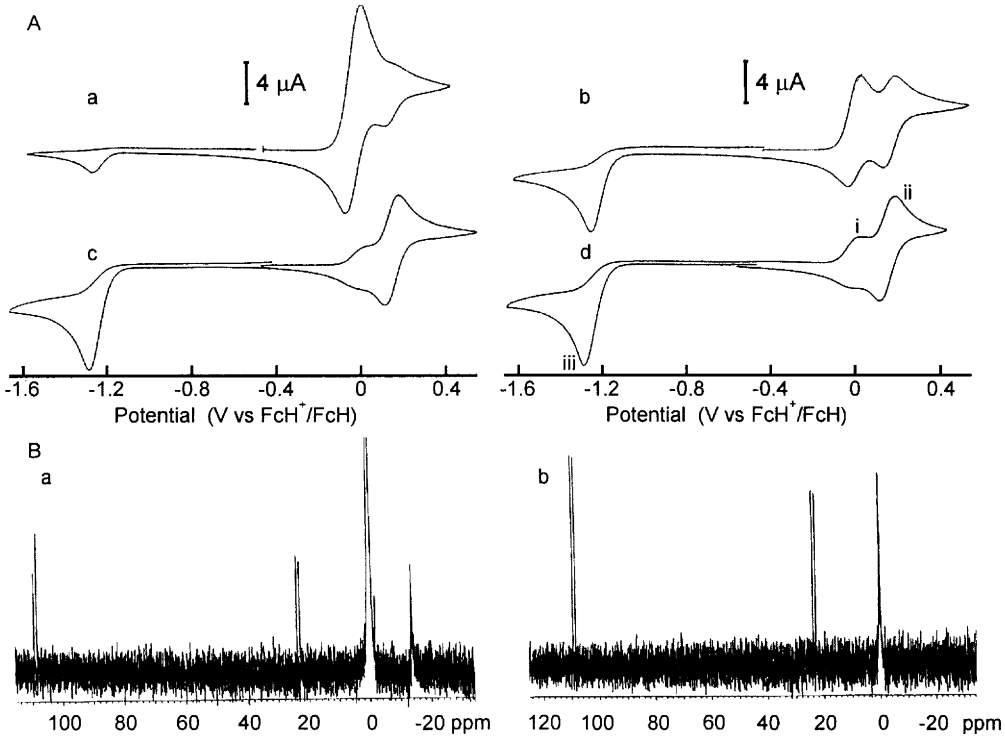

Fig. 5. (A) Cyclic voltammograms obtained using a Pt disk electrode, scan rate = 100 mV s^{-1} in CH_3CN–0.1 M $[Bu_4N]BF_4$ of 5 mM $FcCH_2PPh_2$ (a) before electrolysis, (b) after oxidative electrolysis with charge = 0.5 F mol^{-1} and (c), (d) after oxidative electrolysis with charge = 1.0 F mol^{-1}. (B) ^{31}P NMR spectra of 5 mM $FcCH_2PPh_2$ in CH_3CN–0.1 M $[Bu_4N]BF_4$ (a) after oxidative electrolysis with charge = 0.5 F mol^{-1} and (b) after oxidative electrolysis with charge = 1.0 F mol^{-1}. The solutions were briefly reduced at −0.4 V prior to obtaining spectra.

state voltammograms, the ferrocene centers are converted fully to the neutral form and the solution loses its green tint.

Despite attempts to exactly reproduce experimental conditions, the relative peak currents for processes (i)–(iii) varied significantly between experiments. The currents for processes (ii) and (iii) were similar but the current for couple (i) varied between ca. 10 and 80% that of (ii) (or (iii)). Regardless of these variations, the total current due to oxidation of ferrocene centers in the oxidized solution was approximately half that in the initial solution, as measured by steady-state voltammetry.

Oxidation of the starting compound by 2 F mol^{-1} yields a green solution with the same voltammetric features described above. Consistent with the solution colour, steady-state voltammetry confirms that the ferrocene centers are now in their oxidized form.

Fig. 5B shows the changes in the ^{31}P NMR spectra which accompany the one-electron oxidative bulk electrolysis. There is a progressive loss of the signal due to starting compound ($\delta = -11.8$ ppm vs H_3PO_4) and the growth of two equal-sized doublets at $\delta = 22.7$, 23.6 and 108.2, 109.1 ppm (for each doublet, $J = 118$ Hz). No other signals are seen in the spectrum. After oxidation by a charge corresponding to 1 F mol^{-1}, the spectrum contains only the two doublets (Fig. 5Bb). Note that two doublets of equal intensity are always observed after bulk electrolysis, regardless of the relative sizes of processes (i), (ii) and (iii) in steady-state and cyclic voltammograms.

The voltammograms of Fig. 5Ac and d suggest that the reduction step at −1.25 V may regenerate starting phosphine. Hence solutions which had been oxidized by a charge corresponding to 1 F mol^{-1} were reduced (using controlled current reduction) by a charge corresponding to 1 F mol^{-1}. Voltammetry of the final solutions confirmed formation of a ferrocenylphosphine or ferrocenylphosphine oxide, albeit at lower concentration than the initial ferrocenylphosphine. The steady-state current due to oxidation of ferrocene centers increased compared to the oxidized solution but it was significantly less than that in the starting solution. ^{31}P NMR analysis of the final solutions showed starting ferrocenylphosphine and a variable amount of $FcCH_2P(O)Ph_2$ ($\delta = 29.0$ ppm). There were no other signals. Based on the ^{31}P NMR signals, the amount of the phosphine oxide formed during reduction of the bulk solution varied between experiments from none to ca. 30% that of regenerated starting compound. These results did not appear to depend on the relative currents of redox processes (i), (ii) and (iii) in the oxidized

solution. Even when no $FcCH_2P(O)Ph_2$ was detected in the final solution, cyclic voltammetry showed that recovery of the starting material was close to only 50%.

Voltammetric and ^{31}P NMR analysis of the bulk electrolysis products of $FcCH_2P(CH_2OH)_2$ reveal more complex behaviour for this phosphine after one-electron oxidation (Fig. 6). In addition to oxidation processes at $E_{1/2} \sim -0.05$ and 0.095 V, two broad merged irreversible reduction processes are seen with $E_{pc} = -1.5$ and -1.7 V. ^{31}P NMR analysis of the oxidized solution (Fig. 6c) reveals two doublets (($\delta = 21.9$, 22.7 and 114.8, 115.6 ppm, each with $J = 102$ Hz) and an additional singlet at $\delta = 24.1$ ppm. Reduction of the oxidized solution led to precipitation. After collecting the precipitate and dissolving in DMF, no signals were observed in the ^{31}P NMR spectrum.

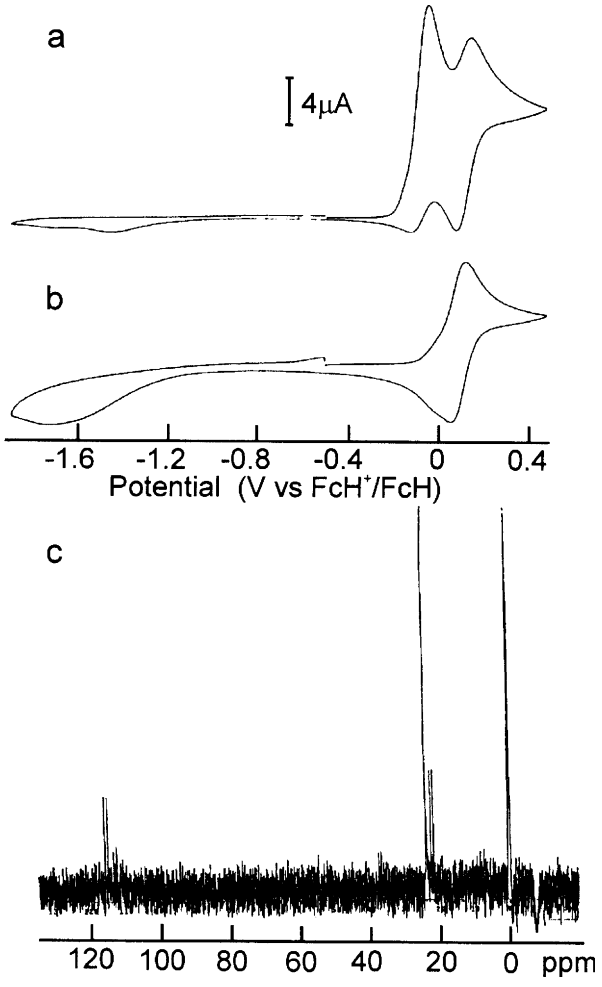

Fig. 6. Cyclic voltammograms (a, b) obtained using a Pt disk electrode, scan rate = 100 mV s^{-1} in CH_3CN–0.1 M $[Bu_4N]BF_4$ of 7.5 mM $FcCH_2P(CH_2OH)_2$ (a) before electrolysis, (b) after oxidative electrolysis with charge = 1.0 F mol^{-1}. (c) ^{31}P NMR spectrum of the solution in (b).

2.6. Chemical oxidation of $FcCH_2PPh_2$ and ESMS and ^1H NMR spectroscopy of oxidation products

Electrochemical monitoring of the reaction of $[FcH]BF_4$ with $FcCH_2PPh_2$ indicated that FcH^+ oxidizes the ferrocenylphosphine leading to the same products as oxidative bulk electrolysis. However, all attempts to isolate reaction products after chemical and electrochemical oxidation were unsuccessful due to the gradual formation of intractable brown decomposition materials. ESMS and ^1H NMR spectroscopy, coupled with chemical oxidation of $FcCH_2PPh_2$, were used to further characterize the oxidation products. ESMS spectra (positive ion mode) were obtained of four samples: FcH, $[FcH]BF_4$, $FcCH_2PPh_2$, and $FcCH_2PPh_2$ mixed with $[FcH]BF_4$. After accounting for signals directly arising from $[FcH]BF_4$ and FcH, the spectra of the latter two samples were very similar. The principal peaks seen in the spectra of samples containing $FcCH_2PPh_2$ were: m/z 199.1 $[FcCH_2]^+$, 384.0 $[2M]^{2+}$, 400.1 $[M+O]^+$, 569.0 $[M+PPh_2]^+$, 783.0 $[2M-H+O]^+$ and 855.1 $[2M+BF_4]^+$. The peaks at m/z 384.0 and 400.1 dominated the spectra.

^1H NMR spectra of acetonitrile solutions of $[FcH]BF_4$ and $FcCH_2PPh_2$ were more complex and less well-resolved than that of the starting ferrocenylphosphine. The phenyl and ferrocenyl signals were shifted downfield, as found for phosphine oxide and phosphonium derivatives. The methylene resonance at 3.2 ppm in $FcCH_2PPh_2$ was absent in spectra of the oxidation products and new singlets appeared at 1.33 and 4.75 ppm. The latter signal could correspond to the methylene resonance shifted downfield by a neighbouring phosphonium center. ^{31}P NMR analysis of the same sample showed the expected doublets and several additional signals which could not be assigned. Hence further analysis of the ^1H NMR spectra was not attempted.

3. Discussion

Voltammetric and ^{31}P NMR analyses of the solutions of $FcCH_2PPh_2$ after oxidation by bulk electrolysis (Fig. 5) suggest formation of product(s) containing at least two types of ferrocene centers (giving redox couples (i) and (ii)) and two types of P centers (giving two doublets in the ^{31}P NMR). The identical NMR P–P coupling constants and the simultaneous formation of both NMR signals (and their simultaneous loss when the oxidized solution is reduced) indicate that the two P environments are in a single molecule. On the other hand there is no evidence for formation of a product containing two ferrocene centers. Based on the voltammetry of the oxidized solutions (Fig. 5A), and the cyclic voltammetry of $FcCH_2P(CH_2OH)_2$ which shows that

the peak current for the oxidation of the product reaches a maximum of half that of the parent compound (Fig. 2d), the product appears to have only one electroactive ferrocene center. After reduction of the bulk oxidized solution, voltammetry is consistent with the regeneration of approximately half the initial amount of starting ferrocenylphosphine while starting material is the only ^{31}P NMR-active compound. Considering these observations we tentatively propose that one ferrocene center is cleaved during formation of the product. The cleaved ferrocenyl moiety may polymerize or undergo other follow-up reactions giving the broad, low current process near 0 V (couple (i), Fig. 5Ad). A polymerization product would account for the broadness of the peaks and the lower total current after reaction. ESMS spectra are consistent with these suggestions showing products arising from a dimerization reaction. However, the very different conditions of the conventional bulk electrolysis and electrospray techniques do not allow firm parallels to be drawn. The alternative possibility that the P–P containing product contains one electroactive ferrocene center and one which is electroinactive cannot be discounted. However, we have no suggestions as to the structure or mechanism of formation of such an electroinactive ferrocene moiety.

On the basis of their potentials and behaviour on reduction, redox couple (ii) and peak (iii) (Fig. 5Ad), and the corresponding processes in voltammograms of the starting ferrocenylphosphine (Fig. 1a), can reasonably be assigned to a ferrocenylphosphonium product. Initial formation of $(R_3P\text{-}PR_3)^+$ or $(R_3P\text{-}PR_3)^{2+}$ after electrochemical oxidation of PR_3 is a well-established reaction pathway [35,36] and hence we propose a P–P bonded phosphonium product which incorporates only one ferrocenyl moiety. An ion with m/z 569.0 in the ESMS spectra is consistent with formation of $FcCH_2P^+R_2PR_2$. However, consideration of the ^{31}P NMR spectra of the reaction products suggests that a simple phosphonium–phosphine species is an unlikely candidate for the final oxidation product. The chemical shifts are not consistent with a phosphine center and the coupling constant is within the range expected for P^V–P^V rather than P^V–P^{III} coupling [37]. A more reasonable product on the basis of the coupling constants is $FcCH_2P^+R_2P(O)R_2$ which could form via reaction with adventitious water. However, while both a phosphonium and phosphine oxide center would be expected to have a chemical shift at the region of the upfield signal of the product, neither can account for the downfield signal. Hence we are unable to confidently assign a structure for the phosphorus center giving rise to the downfield ^{31}P NMR signals.

Considering the suggestion that the reaction pathway involves formation of $FcCH_2P^+R_2PR_2$, the simplest reaction that can account for such a species is shown in Eqs. (1) and (2). Fragmentation to give the ferrocenylmethylene cation $FcCH_2^+$ is a reasonable proposition based on the known of stability of α-ferrocenyl carbocations [38].

$$2[FcCH_2PPh_2]^+ \rightarrow FcCH_2P^+Ph_2PPh_2 + FcCH_2^+ \quad (1)$$

$$FcCH_2^+ \rightarrow \text{follow-up reactions} \quad (2)$$

However, apart from observation of $FcCH_2^+$ in ESMS spectra, there is no direct evidence for the involvement of this species. Likely follow-up reaction products such as bis(ferrocenyl)ethane and $[(FcCH_2)_2PPh_2]^+$ are not detected in NMR or ESMS spectra and hence formation of $FcCH_2^+$ cannot be confirmed.

For $FcCH_2P(CH_2OH)_2$ there is an additional oxidation product to those seen for $FcCH_2PPh_2$ and we propose a ferrocenylphosphonium with an oxidation potential that closely coincides with that of couple (ii), an irreversible reduction process close to that of the P–P product and an NMR signal at δ 24.1 ppm (singlet). This is presumably a species containing either a single P, or two identical P centers.

As the only other ferrocenylphosphine to be subjected to detailed electrochemical investigations, dppf forms an interesting comparison with the compounds described in this work. Since publication of Pilloni et al.'s study of dppf [2], similar electrochemistry has been reported for various ferrocenylphosphines with P directly bonded to the cyclopentadienyl ring and similar reaction pathways have been assumed [8– . Thus, dppf is an important benchmark compound. Pilloni et al. proposed that the redox chemistry of dppf involves an initial one-electron oxidation of the ferrocenyl moiety followed by an intramolecular charge transfer from the P^{III} center. A bimolecular reaction between two $dppf^+$ species leads to the eventual formation of the phosphonium $dppfH^+$ and phosphine oxide dppfO. These species were identified by ^{31}P NMR analysis of the oxidative bulk electrolysis product solution. A dimer, with two P–P bonds, was tentatively proposed as a short-lived intermediate.

For the ferrocenylmethylphosphines of the present study, initial oxidation of the ferrocene center is also proposed and subsequent reactions must involve intramolecular charge transfer from P^{III} giving a reduced (neutral) ferrocene. For these compounds direct evidence for formation of a dimeric species is provided by ^{31}P NMR analysis and is supported by ESMS data. However, reaction of the dimer to give $FcCH_2P^+(H)R_2$ and/or $FcCH_2P(O)R_2$ as primary oxidation products is ruled out by electrochemical and ^{31}P NMR data. The different fate of the initially formed dimeric species for the ferrocenylmethylphosphines is tentatively suggested to be due to the accessibility of $FcCH_2^+$ as a relatively stable cleavage product. Thus, this study lends support to the interpretation of the electrochemistry of dppf and

its analogs and at the same time it has uncovered a new reaction pathway for ferrocenylphosphine ligands.

4. Experimental

4.1. Physical measurements

ESMS was performed in the positive ion mode using a Micromass LCT mass spectrometer with the probe maintained at 3200 V and 150 °C. The source was operated at 80 °C with cone voltage = 20 V. Acetonitrile was used to dissolve samples and as the mobile phase.

^{31}P NMR spectra were acquired on a Varian XL-300 spectrometer operating at 121.45 MHz. Phosphorus chemical shifts are reported relative to external 85% H_3PO_4 at δ 0.0 ppm. For analysis of non-deuterated electrolysis solutions, an external lock signal was provided through use of a D_2O insert. Immediately after acquisition of a sample spectrum, a few transients were obtained from a sample of D_2O containing an 85% H_3PO_4 insert, enabling referencing of the sample. ^{1}H and ^{13}C spectra were recorded on a Bruker AC300 spectrometer operating at 300.13 Hz for ^{1}H and 75.47 Hz for ^{13}C.

All electrochemical experiments were performed in a nitrogen atmosphere at 22 ± 2 °C. Unless stated otherwise, measurements were made in acetonitrile solutions with 0.1 M supporting electrolyte. Identical electrochemical and NMR results were obtained using $[Bu_4N]PF_6$ and $[Bu_4N]BF_4$ electrolytes and these were used interchangeably for voltammetric experiments. Cyclic voltammograms were obtained with a PAR 173 potentiostat with Model 273 interface, a Par Model 175 universal programmer and a Graphtec WX1200 recorder. Working electrodes were GC or Pt disks (area = 7.0 and 0.8 mm^2, respectively) and Pt disk microelectrodes (10 μm diameter). Working electrodes were polished with 1 μm diamond paste prior to obtaining each voltammogram. The auxiliary electrode was a Pt wire and a Ag/Ag$^+$ (0.01 M in CH_3CN–0.1 M $[Bu_4N]PF_6$) reference electrode was used. Potentials are reported vs ferrocenium/ferrocene (FcH^+/FcH) after referencing to ferrocene in a separate solution.

Controlled-potential and controlled-current electrolyses were performed using a PAR Model 273A potentiostat/galvanostat and a three compartment cell. The Pt mesh working and auxiliary electrodes were separated by a porosity 5 glass frit and the working and reference electrodes were separated by a Vycor frit. A nitrogen atmosphere was maintained in the cell and the solution was stirred throughout the electrolysis. Conditions for controlled current electrolyses were: 1 mM ferrocenylphosphine: $I_{app} = 1$ mA; 5 mM ferrocenylphosphine: $I_{app} = 5$ mA.

4.2. Materials

Solvents used for electrochemistry were analytical reagent grade and were dried either by passing through a column of activated neutral alumina or by twice distilling from CaH_2. $[Bu_4N]PF_6$ (Aldrich) was recrystallized from ethanol/water and dried under vacuum at 80 °C. $[Bu_4N]BF_4$ was prepared as described previously [39]. $FcCH_2P(CH_2OH)_2$, $FcCH_2P(O)(CH_2OH)_2$, $FcCH_2P(S)(CH_2OH)_2$, $FcCH_2P(CH_2CH_2CN)_2$ and $FcCH_2PPh_2$, Pt, Pd, Au and Ru complexes of $FcCH_2P(CH_2OH)_2$ and Ru complexes of $FcCH_2PPh_2$ were synthesised as described previously [18,20,24]. $[FcH]BF_4$ was prepared by oxidation of ferrocene with benzoquinone [40].

4.3. Preparation of $FcCH_2P(O)Ph_2$

To a solution of 100 mg (0.26 mmol) of $FcCH_2PPh_2$ in water (5 ml), methanol (35 ml) and dichloromethane (10 ml) was added 190 mg of 6% H_2O_2 (0.335 mmol). After stirring for 1 h solvent was removed under reduced pressure without heating until product precipitated. Diethyl ether was added and the organic layer was washed with water (3 × 10 ml). During washing, sufficient dichloromethane was added to prevent precipitation of the product from the organic layer. Solvent was removed giving the crude product in quantitative yield as a yellow powder. Recrystallization from dichloromethane/petroleum spirits at 4 °C gave the product as a brown powder (86 mg, 0.215 mmol, 83%). Elemental Anal. Found: C, 68.4; H, 5.1%. Calc. for $C_{23}H_{21}FeOP$: C, 69.0; H, 5.3%. $^{31}P\{^1H\}$ NMR ($CDCl_3$): δ 29.0 (s). ^{1}H NMR ($CDCl_3$): δ 3.42 (d, FcCH_2P, J = 13 Hz, 2H), 4.01 (s, 4H, C_5H_4), 4.08 (s, 5H, C_5H_5), 7.39–7.70 (m, 10H, C_6H_5). $^{13}C\{^1H\}$ NMR ($CDCl_3$): δ 33.38 (d, FcCH$_2$P, J = 67 Hz), 68.02 (s, C_5H_4-3), 68.90 (s, C_5H_5), 69.85 (s, C_5H_4-2), 77.77 (d, C_5H_4-1, J = 3 Hz), 128.43 (d, C_6H_5-o, J = 11 Hz), 131.27 (d, C_6H_5-m, J = 9 Hz), 131.76 (s, C_6H_5-p), 133.06 (s, C_6H_5-i).

4.4. Preparation of $[(FcCH_2)_2P(CH_2OH)_2]Cl$

All solution manipulations were carried out in the absence of air in an N_2 atmosphere. $FcCH_2OH$ (0.503 g, 2.33 mmol) was dissolved in 20 ml dry dichloromethane, oxalyl chloride (0.4 ml, 5 mmol) was added and the reaction stirred for 90 min. Solvent was removed under vacuum and the solid redissolved in 20 ml dry dichloromethane. $FcCH_2P(CH_2OH)_2$ (0.681 g, 2.33 mmol) was added and the reaction stirred overnight. The product thus formed was dried under vacuum and methanol (7 ml) added. The slurry was heated to 50 °C, supernatant removed and diethyl ether (40 ml) was used to precipitate the product. After cooling to −30 °C the product precipitated as a yellow microcrystalline solid

(0.354 g, 0.672 mmol, 28.9%). Elemental Anal. Found: C, 54.4; H, 5.4%. Calc. for $C_{24}H_{28}ClFe_2O_2P$: C, 54.7; H, 5.3%. $^{31}P\{^1H\}$ NMR (d^6-DMSO): δ 22.3 (s). ^1H NMR (d^6-DMSO): δ 3.40 (s, 2H, O*H*), 3.52 (d, FcCH_2P, $J =$ 13 Hz, 4H), 4.20 (d, PCH_2O, $J = 6$ Hz, 4H), 4.26 (s, 10H, C_5H_5), 4.27 (unres. t, 4H, C_5H_4), 4.39 (unres. t, 4H, C_5H_4). $^{13}C\{^1H\}$ NMR (d^6-DMSO): δ 21.37 (d, Fc*C*H_2P, $J = 37$ Hz), 54.49 (d, P*C*H_2O, $J = 53$ Hz), 72.41 (s, C_5H_4-3), 72.95 (s, C_5H_5), 73.46 (s, C_5H_4-2), 78.68 (s, C_5H_4-1).

4.5. Preparation of $[FcCH_2P(H)Ph_2]BF_4$

All solution manipulations were carried out in the absence of air in an N_2 atmosphere. To a solution of 100 mg $FcCH_2PPh_2$ (0.26 mmol) dissolved in 5 ml diethyl ether, a solution of HBF_4 in acetonitrile (5.6 ml, 0.27 mmol) was added dropwise with stirring. Petroleum spirits (20 ml) and a small amount of diethyl ether were added, causing the product to separate as an oil. The supernatant was removed and the oil washed with petroleum spirits (3×5 ml), then dried under vacuum for 2 days, giving the product as a yellow oil (0.113 g, 0.239 mmol, 92%). ^{31}P NMR ($CDCl_3$): δ 6.31 (d, ^1J(P–H) = 511 Hz). ^1H NMR ($CDCl_3$): δ 4.57–4.70 (m, 11 H, FcCH_2P, C_5H_5 and C_5H_4), 7.99–8.27 (m, 10H, C_6H_5). $^{13}C\{^1H\}$ NMR ($CDCl_3$): δ 23.82 (d, Fc*C*H_2P, $J = 43$ Hz), 69.55 s, C_5H_4-3), 69.89 (s, C_5H_5), 70.03 (s, C_5H_4-2), 78.15 (d, C_5H_4-1, $J = 611$ Hz), 115.43 (d C_6H_5-*i*, $J = 82$ Hz), 130.20 (d, C_6H_5-*o*, $J = 13$ Hz), 133.67 (d, C_6H_5-*m*, $J = 10$ Hz), 135.14 (s, C_6H_5-*p*).

4.6. Preparation of $[FcCH_2P(Bz)(CH_2OH)_2]Br$

A solution of 100 mg of $FcCH_2P(CH_2OH)_2$ dissolved in methanol (10 ml) was heated to 45 °C and benzyl bromide (0.20 ml, 1.7 mmol) was added dropwise with stirring. Solvent was removed under reduced pressure leaving a yellow oil which gave the crude product as a yellow powder after treatment with methanol/diethyl ether at −30 °C (0.075 g, 0.165 mmol, 49%). $^{31}P\{^1H\}$ NMR (d^6-DMSO): δ 26.0 (s). $^{13}C\{^1H\}$ NMR (d^6-DMSO): δ 19.41 (d, P*C*H_2Bz, $J = 38$ Hz), 23.93 (d, Fc*C*H_2P, $J = 38$ Hz), 52.37 (d, P*C*H_2O, $J = 55$ Hz), 70.32 (s, C_5H_4-3), 70.81 (s, C_5H_5), 71.23 (s, C_5H_4-2), 78.31 (s, C_5H_4-1), 129.75 (s, C_6H_5-*p*), 130.07 (d, C_6H_5-*i*, $J = 8$ Hz), 130.87 (s, C_6H_5-*m*), 139.91 (d, C_6H_5-*o*, $J = 5$ Hz).

Acknowledgements

We thank Rewi Thompson and Bruce Clark for NMR and ESMS measurements, respectively.

References

[1] A. Togni, T. Hayashi (Eds.), Ferrocenes: Homogeneous Catalysis, Organic Synthesis, Materials Science, VCH, Weinheim, 1995.
[2] G. Pilloni, B. Longato, B. Corain, J. Organomet. Chem. 420 (1991) 57.
[3] J.C. Kotz, C.L. Nivert, J. Organomet. Chem. 52 (1973) 387.
[4] T.M. Miller, K.J. Ahmed, M.S. Wrighton, Inorg. Chem. 28 (1989) 2347.
[5] C.E. Housecroft, S.M. Owen, P.R. Raithby, B.A.M. Shaykh, Organometallics 9 (1990) 1617.
[6] B. Corain, B. Longato, G. Favero, D. Ajo, G. Pilloni, U. Russo, F.R. Kreissl, Inorg. Chim. Acta 157 (1989) 259.
[7] D.L. DuBois, C.W. Eigenbrot, Jr., A. Miedaner, J.C. Smart, R.C. Haltiwanger, Organometallics 5 (1986) 1405.
[8] J. Podlaha, P. Stepnicka, J. Ludvik, I. Cisarova, Organometallics 15 (1996) 543.
[9] P. Stepnicka, I. Cisarova, J. Podlaha, J. Ludvik, M. Nejezchleba, J. Organomet. Chem. 582 (1999) 319.
[10] I.R. Butler, M. Kalaji, L. Nehrlich, M. Hursthouse, A.I. Karaulov, K.M.A. Malik, J. Chem. Soc. Chem. Commun. (1995) 459.
[11] P. Zanello, A. Cinquantini, M. Fontani, M. Giardiello, G. Giorgi, C.R. Landis, B.F.M. Kimmich, J. Organomet. Chem. 637–639 (2001) 800.
[12] P. Zanello, G. Opromolla, G. Giorgi, G. Sasso, A. Togni, J. Organomet. Chem. 506 (1996) 61.
[13] A. Gref, P. Diter, D. Guillaneux, H.B. Kagan, New J. Chem. 21 (1997) 1353.
[14] D.A. Durfey, R.U. Kirss, M.R. Churchill, K.M. Keil, W. Feighery, Synth. React. Inorg. Met. Org. Chem. 32 (2002) 97.
[15] A. Masson-Szymczak, O. Riant, A. Gref, H.B. Kagan, J. Organomet. Chem. 511 (1996) 193.
[16] R. Horikoshi, T. Mochida, R. Torigoe, Y. Yamamoto, Eur. J. Inorg. Chem. (2002) 3197.
[17] P. Stepnicka, R. Gyepes, O. Lavastre, P.H. Dixneuf, Organometallics 16 (1997) 5089.
[18] N.J. Goodwin, W. Henderson, B.K. Nicholson, Inorg. Chim. Acta 295 (1999) 18.
[19] N.J. Goodwin, W. Henderson, B.K. Nicholson, J. Fawcett, D.R. Russell, J. Chem. Soc. Dalton Trans. (1999) 1785.
[20] N.J. Goodwin, W. Henderson, B.K. Nicholson, J.K. Sarfo, J. Fawcett, D.R. Russell, J. Chem. Soc. Dalton Trans. (1997) 4377.
[21] N.J. Goodwin, W. Henderson, B.K. Nicholson, J. Chem. Soc. Chem. Commun. (1997) 31.
[22] N.J. Goodwin, W. Henderson, J.K. Sarfo, J. Chem. Soc. Chem. Commun. (1996) 1551.
[23] T.V.V. Ramakrishna, A.J. Elias, A. Vij, J. Organomet. Chem. 602 (2000) 125.
[24] N.J. Goodwin, W. Henderson, Polyhedron 17 (1998) 4071.
[25] E.M. Barranco, O. Crespo, M.C. Gimeno, A. Laguna, P.G. Jones, B. Ahrens, Inorg. Chem. 39 (2000) 680.
[26] T.V.V. Ramakrishna, A.J. Elias, J. Organomet. Chem. 637–639 (2001) 382.
[27] K. Muralidharan, N.D. Reddy, A.J. Elias, Inorg. Chem. 39 (2000) 3988.
[28] M.E.N.P.R.A. Silva, A.J.L. Pombeiro, J.J.R. Frausto da Silva, R. Hermann, N. Deus, T.J. Castilho, M.F.C.G. Silva, J. Organomet. Chem. 421 (1991) 75.
[29] R.D. Eagling, J.E. Bateman, N.J. Goodwin, W. Henderson, B.R. Horrocks, J. Chem. Soc. Dalton Trans. (1998) 1273.
[30] M. Rudolph, D.P. Reddy, S.W. Feldberg, Anal. Chem. 66 (1994) 589A.
[31] H. Maeda, H. Ohmori, Acc. Chem. Res. 32 (1999) 72.

[32] K.S.V. Santhanam, Chem. Organophosphorus Compd. 1 (1990) 103.
[33] R.F. Winter, G. Wolmershauser, J. Organomet. Chem. 570 (1998) 201.
[34] J.E. Kingston, L. Ashford, P.D. Beer, M.G.B. Drew, J. Chem. Soc. Dalton Trans. (1999) 251.
[35] W.B. Gara, B.P. Roberts, J. Chem. Soc. Perkin Trans. 2 (1978) 150.
[36] E.V. Nikitin, A.S. Romakhin, V.A. Zagumennov, Y.A. Babkin, Electrochim. Acta 42 (1997) 2217.
[37] K.R. Dixon, in: J. Mason (Ed.), Multinuclear NMR, Plenum Press, New York, 1987, p. 369.
[38] J.J. Dannenberg, M.K. Levenberg, J.H. Richards, Tetrahedron 29 (1973) 1575.
[39] A.J. Downard, Langmuir 16 (2000) 9680.
[40] N.G. Connelly, W.E. Geiger, Chem. Rev. 96 (1996) 877.